

# Exciton recombination dynamics in an ensemble of (In,Al)As/AlAs quantum dots with indirect band-gap and type-I band alignment

T. S. Shamirzaev,<sup>1</sup> J. Debus,<sup>2</sup> D. S. Abramkin,<sup>1</sup> D. Dunker,<sup>2</sup> D. R. Yakovlev,<sup>2,3</sup> D. V. Dmitriev,<sup>1</sup> A. K. Gutakovskii,<sup>1</sup> L. S. Braginsky,<sup>1</sup> K. S. Zhuravlev,<sup>1</sup> and M. Bayer<sup>2</sup>

<sup>1</sup>*A.V. Rzhanov Institute of Semiconductor Physics, Siberian branch of the Russian Academy of Sciences, RU-630090 Novosibirsk, Russia*

<sup>2</sup>*Experimentelle Physik 2, Technische Universität Dortmund, D-44227 Dortmund, Germany*

<sup>3</sup>*A.F. Ioffe Physical Technical Institute, Russian Academy of Sciences, RU-194021 St. Petersburg, Russia*

(Received 14 July 2011; published 20 October 2011)

The dynamics of exciton recombination in an ensemble of indirect band-gap (In,Al)As/AlAs quantum dots with type-I band alignment is studied. The lifetime of confined excitons that are indirect in momentum space is mainly influenced by the sharpness of the heterointerface between the (In,Al)As quantum dot and the AlAs barrier matrix. Time-resolved photoluminescence experiments and theoretical model calculations reveal a strong dependence of the exciton lifetime on the thickness of the interface diffusion layer. The lifetime of excitons with a particular optical transition energy varies because this energy is obtained for quantum dots differing in size, shape, and composition. The different exciton lifetimes, which result in photoluminescence with nonexponential decay obeying a power-law function, can be described by a phenomenological distribution function  $G(\tau)$ , which allows one to fit the photoluminescence decay with one parameter only.

DOI: [10.1103/PhysRevB.84.155318](https://doi.org/10.1103/PhysRevB.84.155318)

PACS number(s): 78.67.Hc, 78.55.Cr, 68.35.Ct, 78.47.jd

## I. INTRODUCTION

The kinetics of exciton recombination in semiconductor quantum dots (QDs) is often analyzed in terms of an exponential decay with one characteristic recombination time.<sup>1</sup> However, the luminescence decay in QDs is typically nonexponential,<sup>1-3</sup> for which there are several reasons, such as the contribution of dark excitons to the emission or the influence of Coulomb correlation effects. Nevertheless, for a single QD in the strong confinement regime the bright exciton photoluminescence (PL) is found to decay monoexponentially.<sup>2,4</sup> For an ensemble of such QDs, on the other hand, nonexponential decays are often found and a statistical analysis of the time-resolved emission demonstrates that this behavior can be attributed to a dispersion of radiative and/or nonradiative lifetimes of QD confined excitons.<sup>3,5</sup> This ensemble decay at a specific energy results from the superposition of monoexponential PL decays of excitons that are localized in QDs having different sizes, shapes, and compositions.<sup>6</sup> In the case of continuously distributed lifetimes  $\tau$  of excitons, which are characterized by the same recombination energy, their PL decay can be described by a distribution function  $G(\tau)$ .

We demonstrated recently that a nonexponential long-time decay of the exciton PL is characteristic of indirect band-gap (In,Al)As/AlAs QDs with type-I band alignment.<sup>7,8</sup> In these structures the conduction-band minimum is around the  $X$  valley, while the valence-band maximum is around the  $\Gamma$  point. In QDs the momentum is no longer a good quantum number, but the wave function is distributed in momentum space over a range of  $\mathbf{k}$  vectors that is inversely proportional to the quantum-dot size. This extension, however, is still much smaller than the separation in  $k$ -space between the  $\Gamma$  and the  $X$  valley, so the indirect character of the band gap is maintained. As a result, direct band-to-band transitions of electrons resulting in an emission of a photon are strongly suppressed. Instead, the radiative recombination requires the involvement of scattering by phonons or at the heterointerface,

as has been demonstrated in indirect band-gap GaAs/AlAs and InAs/AlAs quantum wells.<sup>9,10</sup> For (In,Al)As/AlAs QDs it has been ascertained that the radiative exciton recombination is mainly caused by the scattering at the heterointerface between the (In,Al)As QD and AlAs matrix.<sup>11,12</sup> Hence the exciton recombination dynamics, namely, the recombination time  $\tau$  and the lifetime distribution  $G(\tau)$ , can yield valuable information on this interface.

In this paper the dynamics of the exciton recombination in ensembles of indirect band-gap (In,Al)As/AlAs QDs with varying sharpness of the QD-matrix interface is studied by time-resolved PL. We demonstrate that the radiative lifetime of the exciton that is indirect in momentum space is strongly influenced by this sharpness. The decay can be well described by a power-law function  $I(t) \sim (1/t)^\alpha$ , which can be accounted for by a phenomenological distribution function  $G(\tau)$  based on a single fitting parameter.

## II. SAMPLES AND EXPERIMENT

The studied self-assembled (In,Al)As QDs, embedded in an AlAs matrix, were grown by molecular-beam epitaxy (Riber-32P system) on semi-insulating (001)-oriented GaAs substrates. The structures had one QD sheet sandwiched between 50-nm-thick AlAs layers grown on top of a 200-nm-thick GaAs buffer layer. The nominal amount of deposited InAs was about 2.5 monolayers. A 20-nm-thick GaAs cap layer protected the AlAs layer against oxidation.

Recently, we demonstrated that the diameter, density, and composition of (In,Al)As/AlAs QDs are determined by the growth conditions such as substrate temperature  $T_g$  and growth interruption time  $t_{GI}$ .<sup>11</sup> Three structures  $S1$ ,  $S2$ , and  $S3$  were grown for this study using the conditions listed in Table I. According to these conditions the structures have different (In,Al)As QD alloy compositions.<sup>11</sup> However, as shown repeatedly, despite the intermixing on the QD composition during the epitaxy, as-grown self-assembled QDs have a sharp

TABLE I. Growth parameters and annealing temperatures for the (In,Al)As/AIAs QDs studied. The average diameter  $D_{av}$ , diameters corresponding to the smaller  $D_S$  and larger  $D_L$  half-width of the QD-size distribution, the QD density, the size dispersion  $S_D$ , and the composition of the (In,Al)As/AIAs QDs are given as well. Additionally, the exponent of the PL decay curve  $\alpha$  and the parameter  $\tau_0$  in the exciton lifetime distribution described by Eq. (3) are listed. Note that the relation  $\gamma = \alpha + 1$  defines another parameter of the exciton lifetime distribution  $\gamma$ . For the structure S2 the diameter corresponding to the larger half maximum in the QD-size distribution is related to QDs with a direct band gap. In order to have for structure S2 an additional ensemble of indirect band-gap QDs with a characteristic diameter being different from  $D_{av}$  and  $D_S$ , we choose the diameter (marked in Fig. 1 by  $D_L^* = 17$  nm) that is related to indirect band-gap QDs. The parameter values marked in the table with an asterisk belong to the QD ensemble with the characteristic diameter  $D_L^*$ .

Structure	$T_g/t_{GI}$ (°C/s)	$T_{an}$ (°C)	$D_S$ (nm)	$D_{av}$ (nm)	$D_L$ (nm)	QD density ( $\times 10^{10}$ cm $^{-2}$ )	$S_D$ (%)	Average fraction of InAs in QDs	$\tau_0$ (ns)/ $\alpha$		
									$I_{1/2}(D_S)$	$I_{max}(D_{av})$	$I_{1/2}(D_L)$
S1	450/10	–	4.3	$5.5 \pm 0.21$	7	10	40	0.99	130/1.75	100/1.75	70/1.30
S2	460/60	–	9	$13.8 \pm 0.22$	17*	8.5	60	0.80	240/1.95	130/1.55	60*/1.25*
S3	510/60	700	15	$18.3 \pm 0.15$	22	4.2	52	0.47	2300/1.75	2100/1.50	700/1.35
S4	460/60	800	12	$19.6 \pm 0.16$	28	8.5	75	0.35	5400/2.45	5200/2.40	4000/2.08

QD-matrix interface.<sup>13,14</sup> The reason for the sharp interface formation arises from the Stranski-Krastanov growth mode. The QD composition is determined by the intermixing during the dot formation due to mass transfer along the wetting layer.<sup>15–17</sup> The interfaces of QDs that are independent of their composition are given by stable crystallographic planes, which ensure minimization of the interface energy. These planes provide interface stability against the intermixing with the matrix material during the overgrowth of the QDs. Nevertheless, the sharpness of the (In,Al)As/AIAs interfaces can be smeared out by means of high-temperature postgrowth thermal annealing.<sup>18</sup> Two of the structures studied S2 and S3 were annealed for 1 min at elevated temperatures  $T_{an}$ . Data on  $T_{an}$  are listed in Table I, whereas technical details can be found in Ref. 18. In the following we will refer to the annealed S2 structure as the S4 structure.

The QD size and density are studied by transmission electron microscopy (TEM) using a JEM-4000EX system operated at an acceleration voltage of 250 keV. From the TEM images we find that the self-assembled (In,Al)As QDs are lens shaped with a typical aspect ratio (height to diameter) of 1:4.<sup>8</sup> TEM plane-view images and the respective histograms of the QD-diameter distribution are shown in Fig. 1 for all structures. The average diameters  $D_{av}$  and the diameters corresponding to the larger  $D_L$  and smaller  $D_S$  half-widths of the QD-size distribution obtained from the TEM images are summarized in Table I. Additionally, the size dispersion  $S_D$  is listed, which is defined by the ratio of the half-width of the Gaussian distribution of QD sizes to the average diameter  $S_D = 100\% \times (D_L - D_S)/D_{av}$ .

The unannealed structure S1 has a relatively narrow distribution ( $S_D = 40\%$ ) around a small QD size of  $D_{av} = 5.5$  nm. The structures S2, S3, and S4 contain QDs with larger diameters, which are also distributed over broader ranges. The largest lateral QD sizes are found for the structure S4, which was annealed at the highest temperature of 800 °C. The comparison between the annealed structure S4 and the unannealed structure S2 indicates that postgrowth annealing leads to an increase of the QD diameter with a broader distribution, in good agreement with previous results.<sup>18</sup> The annealing results in an increase of the average QD diameter from 13.8 to 19.6 nm and  $S_D$  from 60% to 75%, respectively.

The diameter increase by annealing is a result of InAs diffusion from the QD into the surrounding AIAs matrix. Therefore, the annealing results in the appearance of a diffused  $In_xAl_{1-x}$ As layer around the QD-matrix interface. It is obvious that the thickness of this  $In_xAl_{1-x}$ As layer depends on the annealing temperature and duration. The sharpness of the interface is defined as the degree of spatial separation between the different materials of (In,Al)As and AIAs. Thus the sharpness of the QD-matrix interface can be described in terms of the thickness of this diffused layer: A sharp (blurred) interface corresponds to a thin (thick)  $In_xAl_{1-x}$ As layer. Therefore, the structures S1–S4 provide us with a representative set of QD ensembles having different diameters and interface sharpness.

The steady-state and time-resolved PL measurements were performed at a temperature of  $T = 5$  K. For excitation of the steady-state PL a He-Cd laser with a photon energy of 3.81 eV was used. The time-resolved PL experiments were established by the third harmonic of a Q-switched Nd:YVO<sub>4</sub> laser (3.49 eV) with a pulse duration of 5 ns. The pulse-repetition frequency was varied from 1 to 100 kHz and the pulse energy density was chosen between 0.04 and 12  $\mu$ J/cm<sup>2</sup>. The light emitted was dispersed by a 0.5-m monochromator and detected by a GaAs photomultiplier operating in the time-correlated photon-counting mode. In order to monitor the PL decay in a wide temporal range up to 0.5 ms the time resolution of the detection system was varied between 1.6 and 200 ns.

### III. EXPERIMENTAL RESULTS

#### A. Steady-state photoluminescence

Normalized PL spectra of the structures studied are shown in Fig. 2. Two PL bands DQD and IQD are observed in the spectra. Recently, we showed that the PL kinetics of the DQD and IQD bands are considerably different. The DQD and IQD bands result from exciton recombination in QDs with direct and indirect band gaps, respectively. It has been evidenced by pulsed excitation measurements that the intensity of the DQD emission band drops quickly with a decay time shorter than 20 ns, while the IQD band decays nonexponentially over hundreds of microseconds.<sup>8</sup> These two types of QDs coexist in these ensembles of (In,Al)As/AIAs QDs.<sup>8,11</sup> For the PL spectra

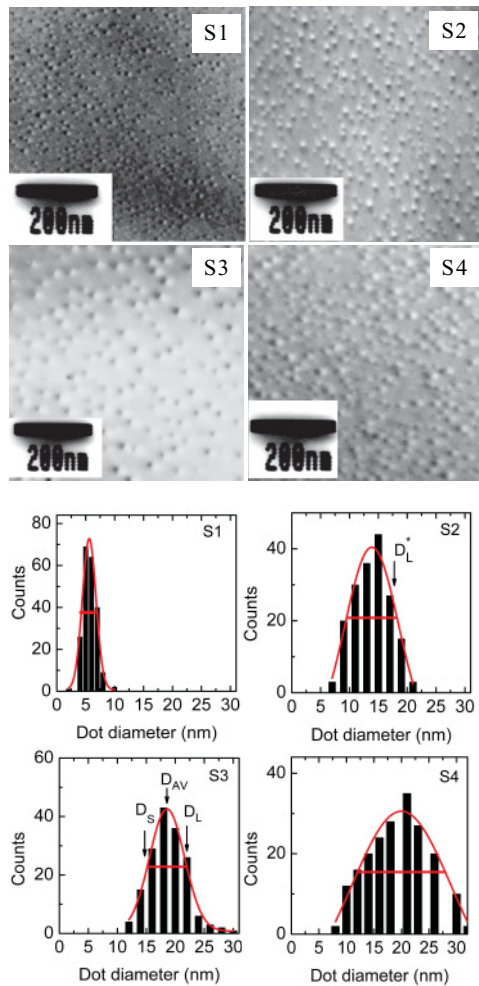


FIG. 1. (Color online) TEM plane-view images (top panels) and histograms of the QD-diameter distribution (lower panels), including the size dispersion fitted by Gaussian curves for the structures S1–S4. The histograms show the incidences of finding a QD with a specific diameter in a TEM image within an area ranging from 0.3 to 0.5  $\mu\text{m}^2$ . The half-widths of the QD-size distribution are marked by the horizontal lines. The average diameter  $D_{av}$  and the large- $D_L$  and small- $D_S$  half-widths of the QD-size distribution are indicated for the structure S3. For the structure S2,  $D_L^*$  is taken as the diameter corresponding to indirect band-gap QDs (see caption to Table I).

of the S1, S2, and S3 structures the direct DQD band has been observed at energies below 1.65 eV. This energy coincides with the observed and calculated boundary between the direct and indirect band-gap (In,Al)As/AlAs QDs.<sup>8,11</sup>

Since the shape of the PL emission reflects the distribution of QD sizes, we establish in the following the relation between the parameters characterizing the spectra and the geometric quantities of the average diameter  $D_{av}$  and size dispersion  $S_D$ . This relation is given by the following features.

(a) The increase of  $D_{av}$  and  $S_D$  for the as-grown structures S1 and S2 leads to a low-energy shift from 1.8 to 1.7 eV and an increase in the full width at half maximum (FWHM) of the IQD band from 115 to 195 meV, respectively. Additionally, the intensity of the DQD band is increased by one order of magnitude in S2 compared to S1.

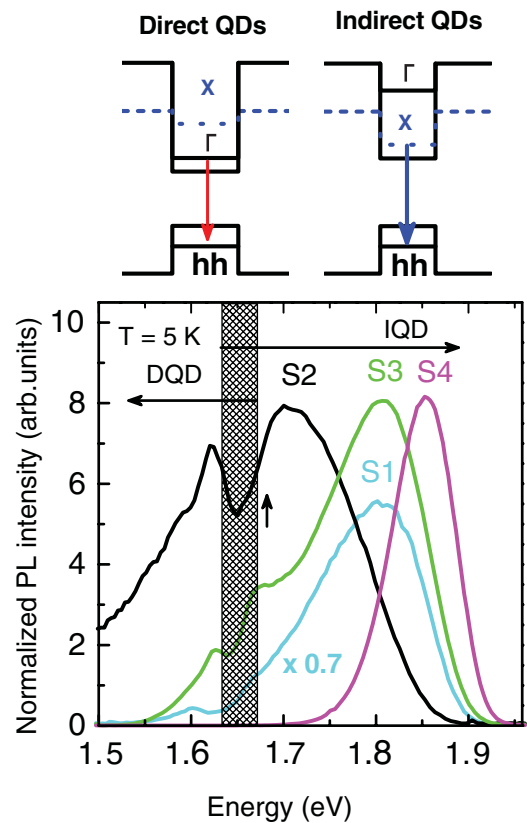


FIG. 2. (Color online) Normalized PL spectra of the different (In,Al)As/AlAs QD structures S1–S4, excited by a He-Cd laser with a power density of 10 W/cm<sup>2</sup>. The PL intensity of the S1 structure is multiplied by a factor of 0.7 for better visibility. The vertical dotted area marks the boundary between the emission from QD excitons either direct or indirect in momentum space as calculated in Refs. 8 and 11. The vertical arrow indicates the energy of exciton recombination in QDs with a typical diameter  $D_L^*$  for the structure S2 (see the caption of Table I). Schemes on top: Real-space band structures of direct- and indirect-band-gap QDs, including the energetically lowest  $\Gamma$  and X conduction-band states as well as the heavy-hole (hh) states.

(b) The increase in  $D_{av}$  and  $S_D$  as a result of high-temperature annealing of the S2 structure and its transformation to the S4 structure leads, for the IQD band, to a high-energy shift from 1.7 to 1.85 eV and a decrease of the FWHM from 195 to 75 meV. The annealing results also in a decrease of the DQD band intensity in the S3 structure and the disappearance of such a band in the S4 structure.

In order to explain the results obtained we have to take into account that the energy of the optical transition is determined by two factors: (i) the quantum confinement energy, which decreases with increasing QD size, and (ii) the band-gap energy of the (In,Al)As alloy in the QD, which increases with a decreasing InAs fraction. In lens-shaped QDs the confinement energy is mainly determined by the QD height. The average QD composition can be evaluated from a comparison of the IQD band energy position with results of model calculations.<sup>19</sup> The determined QD compositions are collected in Table I.

A comparison of the observed optical transition energy with calculations shows that the low-energy shift and broadening of

the IQD band, going from the  $S1$  to the  $S2$  structure, are caused by a decrease in quantum confinement and an increase in the size dispersion  $S_D$ , while the change in the QD composition is negligible. On the other hand, the high-energy shift of the IQD band for the  $S4$  structure compared to  $S2$  is due to an increase of the (In,Al)As alloy band-gap energy with decreasing InAs fraction in the QD alloy composition. This compensates for the decrease in quantum confinement energy due to the annealing-induced increase of the QDs height based on a fixed aspect ratio. The seemingly unusual reduction of the FWHM of the IQD band with increasing  $S_D$  was explained in our previous study.<sup>18</sup>

We calculated in Refs. 8 and 11 the energy separation between the optical transitions of direct and indirect excitons and showed that it weakly depends on the QD size, shape, and composition. Therefore, the change in the relative intensity of the DQD band reflects the change in the relative layer density of the direct-band-gap QDs. This density is a function of the QD size and composition. The disappearance of the DQD band in the emission of the  $S4$  structure results from the lower InAs fraction in the QD alloy composition. This in turn gives rise to a conversion of the band gap from a direct to an indirect one.

### B. Time-resolved photoluminescence

For direct-band-gap (In,Ga)As QDs with typical exciton lifetimes of about 1 ns the condition that the QD exciton population does not exceed one exciton can be easily established. As an example, for (In,Ga)As/GaAs QD ensembles, which are excited by picosecond pulses (at 13.2-ns pulse separation), the average exciton population per dot is smaller than 0.15, when an average excitation density of  $8 \text{ W/cm}^2$  (with an energy density of  $100 \text{ nJ/cm}^2$  per pulse) is used.<sup>2</sup>

However, in indirect-band-gap QDs with long exciton lifetimes the optical excitation has to be carefully chosen in order to avoid accumulation of electron-hole pairs and formation of multiexciton complexes in the QDs. For that purpose, specific experimental conditions need to be established. The number of excitons, which are photogenerated in the QD surrounding matrix and captured in the QDs per laser pulse, is mainly determined by the pulse energy density, but is independent of the QD band-gap structure because the relaxation from the excited  $\Gamma$  to the  $X$  ground state is very fast. The repetition frequency of the excitation pulses should be reduced to a level that there is sufficient time for the excitons to recombine between subsequent pulses, so that multiexciton complexes are not created. Since the lifetime of the indirect excitons in the (In,Al)As/AlAs QDs exceeds that of direct excitons in (In,Ga)As/GaAs QDs by up to five orders of magnitude,<sup>8</sup> the pulse-repetition frequency as well as the average excitation density should decrease correspondingly. To ensure that we actually study the recombination dynamics of single excitons in the (In,Al)As/AlAs QDs, the PL kinetics was measured at different excitation densities and repetition frequencies.

Figure 3 shows low-temperature PL kinetics measured at the IQD band maximum of the  $S4$  structure for different excitation pulse energy densities. The kinetics of the other structures is similar to the one presented. The transient PL data are plotted on a double-logarithmic scale, which is convenient to illustrate the nonexponential character of the decay over

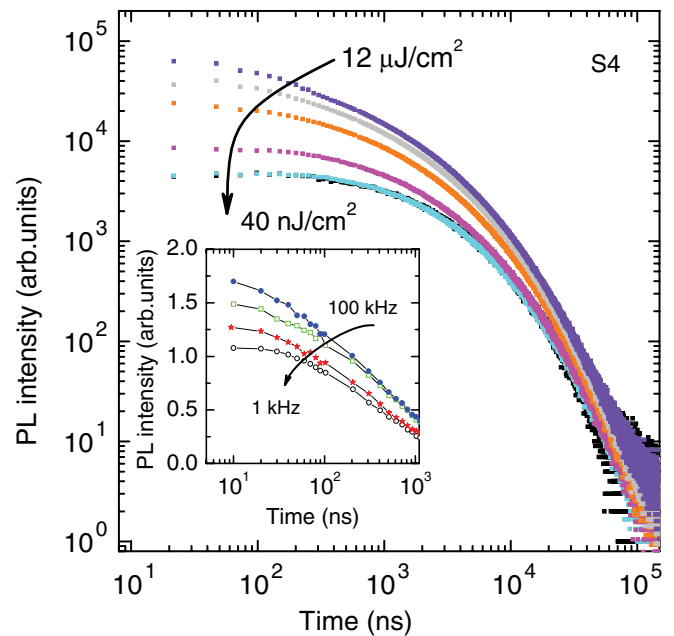


FIG. 3. (Color online) Low temperature ( $T = 5 \text{ K}$ ) PL kinetics obtained at the maximum of the IQD band ( $1.856 \text{ eV}$ ) for the  $S4$  structure using different energy densities of the excitation pulse (note the double-logarithmic scale). The excitation pulse ends at  $t = 10 \text{ ns}$ . The pulse-repetition frequency is  $1.5 \text{ kHz}$ , which is sufficiently low to monitor a PL intensity decrease by five orders of magnitude between successive laser pulses. The excitation pulse densities  $P$  (given in  $\text{nJ/cm}^2$ ) are, from top to bottom,  $1.2 \times 10^4$ ,  $4 \times 10^3$ ,  $1.2 \times 10^3$ ,  $400$ ,  $120$ , and  $40$ . The inset demonstrates the PL kinetics measured at  $P = 900 \text{ nJ/cm}^2$  for different pulse-repetition frequencies from top to bottom (in kHz):  $100$ ,  $30$ ,  $10$ , and  $1$ . While for the power density a logarithmic scale is again chosen, the intensity axis is scaled linearly in order to underline the changes in the PL decay.

a wide range of times and PL intensities. The recombination kinetics demonstrates two distinctive stages: (i) a relatively flat PL decay immediately after the excitation pulse up to approximately  $1 \mu\text{s}$  and, subsequently, (ii) a reduction in the PL intensity, which can be described by a power-law function  $I(t) \sim (1/t)^\alpha$ , as shown in our previous studies.<sup>7</sup> One can see that in the case of stage (i), a high-power excitation results in a fast decay of the exciton PL. It can be assigned to the recombination of multiexciton complexes.<sup>4</sup> By decreasing the power down to  $P = 120 \text{ nJ/cm}^2$  the decay decelerates; below this power the intensity does not temporally change, thus indicating a saturation level. It is induced by the recombination of single excitons in the QDs. Taking into account the absorption of the laser light in the AlAs matrix<sup>20,21</sup> together with the QD density, the average number of excitons captured in a QD per pulse is estimated to about  $0.3$  for  $P = 120 \text{ nJ/cm}^2$ . An increase in the repetition rate of the excitation pulses at fixed pulse power also results in an acceleration of the initial kinetics stage, as shown in the inset of Fig. 3. As the sample has to be excited by each pulse when it has reached its equilibrium state, for the subsequent studies presented in this paper we select  $P = 40 \text{ nJ/cm}^2$ . This corresponds to an average QD exciton population of  $0.1$  per pulse at a repetition frequency of  $1.5 \text{ kHz}$ , which is



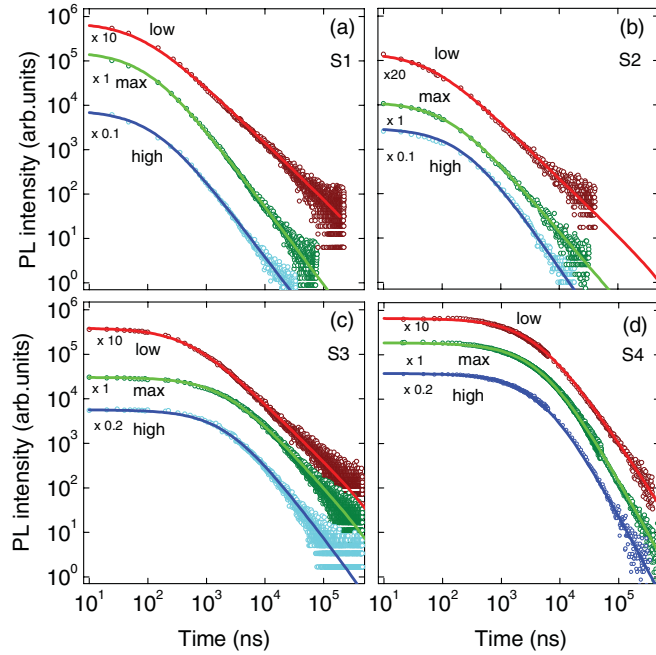


FIG. 4. (Color online) Low-temperature ( $T = 5$  K) PL kinetics measured for the structures  $S1$ – $S4$  at the intensity maximum (max) and at half of this maximum on either the high-energy (high) or the low-energy (low) side of the IQD emission band. The excitation density amounts to  $P = 40$  nJ/cm<sup>2</sup> and the pulse repetition frequency is 1.5 kHz. The excitation pulse ends at 10 ns. The scaling factors of the PL intensities are introduced for better visualization. The thick solid lines show the modeled results with the distribution of  $G(\tau)$  described by Eq. (3) with the parameters presented in Table I. For the  $S2$  structure the curve marked low corresponds to the exciton recombination in QDs with a typical diameter  $D_L^*$ .

equal to a time interval of 670  $\mu$ s between the subsequent pulses.

Figure 4 shows PL decays for the structures  $S1$ – $S4$ , which have been measured at different energies. The selection of different detection energies provides information on the exciton recombination in QDs with different characteristic sizes in the ensemble. The energy of the intensity maximum of the IQD band (the curves labeled max) corresponds to recombination in QDs with the diameter  $D_{av}$  and that of the half maximum (curves labeled high and low) refers to recombination in QDs with diameters  $D_s$  and  $D_L$ , respectively. The following features of the PL decay can be extracted. (i) For each structure the exponent  $\alpha$  of the power-law decay is determined by fitting the second stage of the decay curves with the form  $I(t) \sim (1/t)^\alpha$ , as listed in Table I. The exponent  $\alpha$  increases monotonically across the IQD band from the low- to the high-energy side. (ii) The second decay stage starts 100 ns after the end of the excitation pulse in the unannealed structures  $S1$  and  $S2$ , while for the annealed structures  $S3$  and  $S4$  it begins several microseconds after the pulse.

The PL decay obviously depends on the sample characteristics and as will be shown in the following, it is affected by both the typical QD size in the ensemble and the interface sharpness. To obtain a quantitative description of the effect of QD size and interface sharpness on the exciton lifetime in the (In,Al)As/AlAs QD ensembles, we need to construct the

distribution function  $G(\tau)$ , which controls the observed PL kinetics.

### C. Exciton-lifetime distribution in (In,Al)As/AlAs QD ensembles

Nonexponential decays of the exciton PL intensity  $I(t)$  are frequently described by stretched exponentials of the form  $I(t) \propto \exp[-(t/\tau)^\beta]$ , including a constant lifetime  $\tau$  and a dispersion factor  $\beta$ .<sup>22,23</sup> The stretch parameter  $0 < \beta \leq 1$  qualitatively expresses the underlying distribution function  $G(\tau)$ : A broad distribution results in  $\beta \ll 1$ , while for a narrow one  $\beta$  is about 1. However, the evaluation of the lifetime distribution on the basis of the stretched-exponential model is mathematically complicated and feasible only for specific  $\beta$  values (see Ref. 3 and references therein). Alternatively, the distribution  $G(\tau)$  can be determined using the following equation:

$$I(t) = \int_0^\infty G(\tau) \exp\left(-\frac{t}{\tau}\right) d\tau. \quad (1)$$

Here  $G(\tau)$  is established via either the numerical solution of the integral equation<sup>24–26</sup> [Eq. (1)] or an assumed analytical expression of  $G(\tau)$  with a set of fitting parameters. Recently van Driel *et al.*<sup>3</sup> assumed that the most successful distribution function to model  $G(\tau)$  in a QD ensemble among different analytical expressions such as normal and Lorentzian distributions is a log-normal function given by

$$G(\tau) = \frac{A}{\tau^2} \exp\left(-\frac{\ln(\tau_0/\tau)}{w}\right)^2, \quad (2)$$

with the constant  $A$  and the maximum  $\tau_0$  of the exciton lifetime distribution. The dimensionless parameter  $w$  describes the distribution width  $\Delta_{1/\tau}$  of the inverse recombination times at the  $1/e$  level:  $\Delta_{1/\tau} = \frac{2}{\tau_0} \sinh(w)$ . This distribution was successfully used to describe the nonexponential decay of the exciton PL intensity over two to three orders of magnitude for different QD systems with a continuous distribution of direct exciton lifetimes. Among them are ensembles of CdSe/ZnSe colloidal QDs<sup>27</sup> and dye molecules embedded in a photonic crystal.<sup>28</sup>

Since in (In,Al)As/AlAs QDs the excitons recombine via radiative recombination only,<sup>29</sup> the nonexponential decay is the result of the dispersion of the excitonic radiative times in the ensemble. In order to determine  $G(\tau)$  we follow the approach of Ref. 3 and fit the PL kinetics with Eq. (1) using the log-normal distribution of Eq. (2). Unfortunately, the log-normal distribution does not allow us to describe the PL decay satisfactorily over the whole dynamical range. One could see in Fig. 5, for the structures  $S1$  and  $S4$ , that for the decay curves, measured at a maximum intensity of the IQD band (corresponding to recombination in QDs with diameter  $D_{av}$ ), this distribution allows one to fit either the initial stage (curves 1) or the long-time stage (curves 2) of the decay, using different sets of parameters, which are given in the figure caption.

In order to describe the exciton PL decay in our structures over the whole dynamical range of five orders of magnitude we

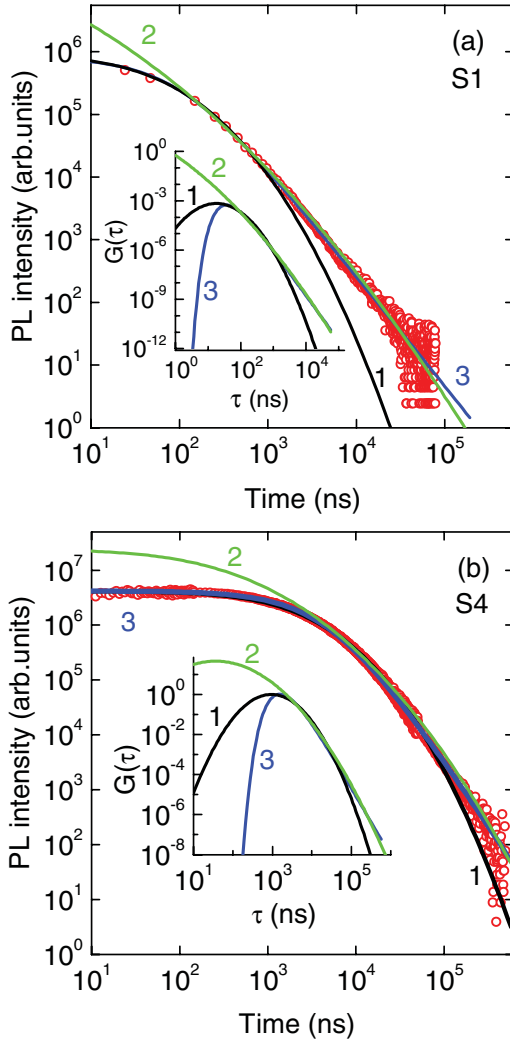


FIG. 5. (Color online) PL decay of the samples *S1* and *S4* of the (In,Al)As/AlAs QDs measured at the IQD band maximum for  $T = 5$  K; the experimental data are shown by circles. The excitation density is  $P = 40$  nJ/cm<sup>2</sup> and the pulse repetition frequency is 1.5 kHz. The end of the excitation pulse corresponds to a time of 10 ns. The modeling of the PL decays by different distribution functions  $G(\tau)$  is shown by the lines. The corresponding distribution functions are given in the insets. (a) Structure *S1*: curves 1 and 2 are based on model calculations using the log-normal distribution  $G(\tau)$  of Eq. (2) with parameter sets  $(\tau_0 = 0.2 \mu\text{s}, w = 1.55)$  and  $(\tau_0 = 0.05 \mu\text{s}, w = 3.50)$ , respectively. Curve 3 is for  $G(\tau)$  of Eq. (3) with the parameters  $\tau_0 = 0.1 \mu\text{s}$  and  $\gamma = 2.75$ . (b) Structure *S4*: curves 1 and 2 are also modeled by  $G(\tau)$  of Eq. (2) with the parameter sets  $(\tau_0 = 5.8 \mu\text{s}, w = 1.35)$  and  $(\tau_0 = 3.0 \mu\text{s}, w = 2.10)$ , respectively. Curve 3 is given by  $G(\tau)$  with  $\tau_0 = 5.2 \mu\text{s}$  and  $\gamma = 3.40$ .

propose a nonsymmetric phenomenological distribution  $G(\tau)$ , which is suitable for fitting power-law decays  $I(t) \sim (1/t)^\alpha$ :

$$G(\tau) = \frac{C}{\tau^\gamma} \exp\left(-\frac{\tau_0}{\tau}\right). \quad (3)$$

Here  $C$  is a constant and  $\tau_0$  characterizes the maximum of the distribution of exciton lifetimes. The parameter  $\gamma$  in Eq. (3) is defined as  $\alpha + 1$ . By use of a double-logarithmic scale the power-law decay  $(1/t)^\alpha$  represents a line with a slope  $\alpha$ . Note

that, with knowledge of the exponent  $\alpha$  of the experimental decay curve, only a single free parameter  $\tau_0$  is required to describe the PL decay by Eq. (3).

We use Eq. (3) to fit the decay curves in Fig. 5. The experimentally determined  $\alpha$  values (see Table I) yield the values of  $\gamma = 2.75$  and 3.40 for the structures *S1* and *S4*, respectively. One could see excellent agreement between the experimental data and the calculations for the whole PL decay comprising five orders of magnitude from the low-nanosecond to the high-microsecond region, shown by the curves 3 in Figs. 5(a) and 5(b). The fits were obtained for  $G(\tau)$  of Eq. (3), depicted in the insets of Fig. 5 by the curves labeled 3. The fit parameters used are  $\tau_0 = 0.1$  and  $5.2 \mu\text{s}$  for the structures *S1* and *S4*, respectively.

Let us now discuss the parameter  $\gamma$  in Eq. (3). The comparison of the distribution functions [Eqs. (2) and (3)], as shown by curves 1 and 3 in the insets of Fig. 5, clearly demonstrates that the strong difference in  $G(\tau)$  for lifetimes smaller than  $\tau_0$  has very little influence on the initial stage of the PL decay ( $\tau_0 \geq t$ ). Thus the decay curves are mainly contributed by recombination of excitons with lifetimes exceeding  $\tau_0$ . Therefore, the value of the parameter  $\gamma$ , which is the exponent of the long-lifetime tail of  $G(\tau)$ , can be used as a qualitative measure for the effective width of the distribution  $G(\tau)$ . According to Eq. (3), an increase in  $\gamma$  reduces the dispersion of the  $\tau$  values that contribute to the long-time tail of the kinetics curve.

We would also like to demonstrate that the filling of the QDs with multiexciton complexes at high excitation densities distorts  $G(\tau)$ . Figure 6 illustrates the  $G(\tau)$  distributions obtained via fitting of the recombination kinetics for the

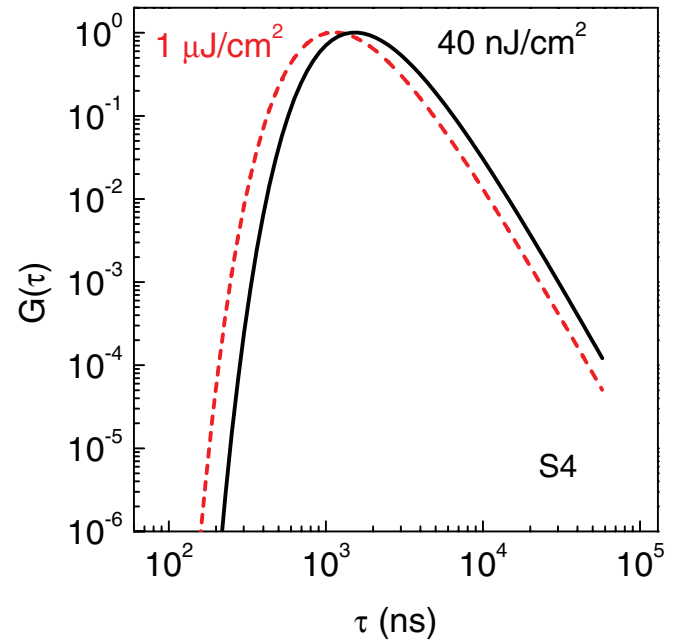


FIG. 6. (Color online) Normalized distribution functions  $G(\tau)$  corresponding to QD ensembles with the same average diameter  $D_{av} = 19.8$  nm (structure *S4*). The two dependences are obtained by fitting the recombination kinetics measured for different excitation energy densities: 40 nJ/cm<sup>2</sup> (black solid line) and 1  $\mu\text{J}/\text{cm}^2$  (red dashed line).

exciton population of less than one ( $40 \text{ nJ/cm}^2$ ) and in the case of multiexciton occupation ( $1 \mu\text{J/cm}^2$ ). One could clearly see in Fig. 6 that multiexciton QD occupation shifts the distribution maximum to shorter times. Thus, in order to reveal  $G(\tau)$ , which is intrinsic for the ensemble of indirect-band-gap QDs, the average exciton population in the dots should be less than unity.

#### D. Effect of interface sharpness on exciton lifetime

Using Eqs. (1) and (3) we determine the  $G(\tau)$  distributions for the four structures studied by fitting the decay curves presented in Fig. 4. The values of the parameters  $\gamma = \alpha + 1$  and  $\tau_0$  resulting from the fitting are collected in Table I. The results of the fitting are shown in Fig. 4 by solid lines.

The following conclusions on the distribution properties can be drawn from the data in Table I.

(i) A monotonic decrease of  $\tau_0$  and  $\gamma$  with increasing QD diameter (from  $D_S$  to  $D_L$ ) is a common feature for each structure.

(ii) The relative change of  $\tau_0$  and  $\gamma$  with changing QD diameter from  $D_S$  to  $D_L$  is larger in the as-grown structures S1 and S2 than in the annealed structures S3 and S4. This is also evidenced by Fig. 7(a) for the structures S2 (with smaller dispersion  $S_D = 60\%$ ) and S4 (with larger dispersion  $S_D = 75\%$ ).

(iii) Despite the larger QD diameters in the annealed structures S3 and S4 than in the as-grown structures S1 and S2,  $\tau_0$  is much smaller in S1 and S2 than in S3 and S4. Also, it is independent of the QD diameter, as demonstrated in Fig. 7(b) for the QDs with their average diameters  $D_{av}$  in structures S1–S4.

These features give us the possibility of distinguishing between the effect of QD size and interface sharpness on the exciton lifetime. One could see in Fig. 7(b) and in Table I that, despite the large difference in QD diameter ( $D_{av} = 5.5$  and  $13.8$  nm for S1 and S2, respectively), these structures have similar distributions of exciton lifetime. On the other hand, the comparison of  $G(\tau)$  in QD ensembles with similar diameters ( $D_L = 17$  nm,  $D_{av} = 18.3$  nm, and  $D_{av} = 19.6$  nm for the structures S2, S3, and S4, respectively) highlights a strong increase of the exciton lifetime with decreasing interface sharpness by about two orders of magnitude. Thus the exciton lifetime in indirect-band-gap (In,Al)As/AlAs QDs is mainly determined by the interface sharpness, while its dependence on the QD size is much weaker. Nevertheless, the monotonic decrease of  $\tau_0$  with increasing QD diameter from  $D_S$  to  $D_L$  for each of the structures studied indicates that the effect of the QD size on the recombination time is also important.

Our theoretical estimations are in accordance with the experimental data. As demonstrated in the Appendix, the lifetime of an exciton that is indirect in momentum space can be described by the form  $\tau \propto \exp(d/a + d/L)$  due to momentum scattering at the interface. Here  $a$  is the lattice constant,  $L$  is the QD height, and  $d$  is the thickness of the diffused (In,Al)As layer at the QD-matrix interface.

Note that the ratio  $d/a \geq 1$  increases with an increase of the thickness  $d$  of the diffused layer. Therefore, the exciton lifetime is mainly determined by  $d/a$ . It is reasonable to assume that  $d/a$  changes weakly with the QD size for

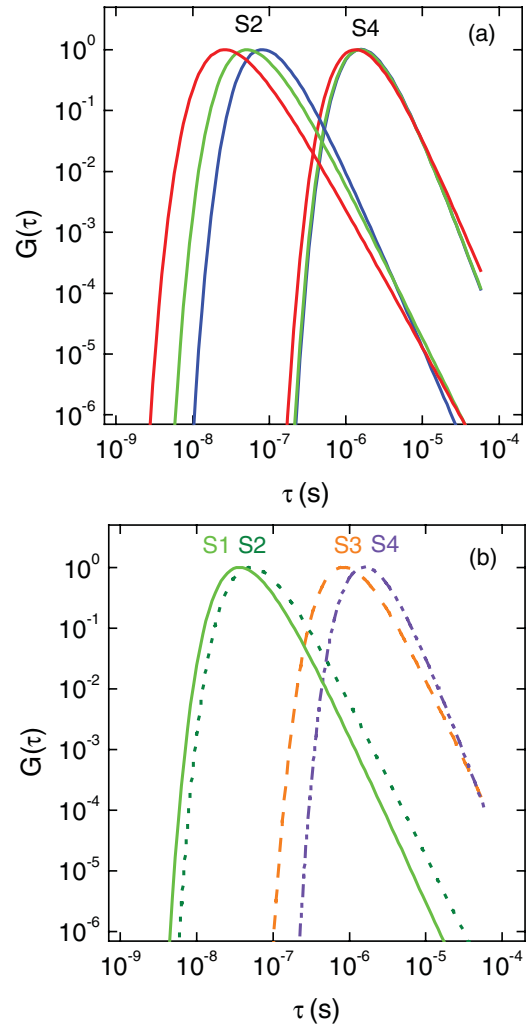


FIG. 7. (Color online) Distributions  $G(\tau)$  corresponding to (a) the QDs with diameters  $D_L = 17$  nm,  $D_{av} = 13.8$  nm, and  $D_S = 9$  nm for structure S2 (from left to right) and the QDs with typical diameters  $D_L = 28$  nm,  $D_{av} = 19.8$  nm, and  $D_S = 12$  nm for structure S4 and (b) the QDs with the diameters  $D_{av} = 5.5$  nm in structure S1,  $D_{av} = 13.8$  nm in structure S2,  $D_{av} = 18.3$  nm in structure S3, and  $D_{av} = 19.6$  nm in structure S4.

a particular structure type. Hence the dependence of the exciton lifetime for such a structure type on the QD size is specified by the second term  $d/L < 1$ . As a result, the exciton lifetime decreases, in agreement with the experimental data, for example, for the S2 structure in Fig. 7(a).

A decrease of the exciton lifetime with an increase in  $d/a$  value is restricted by the rate of phonon emission. When the rate of non-phonon-recombination becomes smaller than that of the phonon emission the exciton recombination is mainly determined by the phonon emission. Actually, we demonstrate in Ref. 18 that a very high annealing temperature ( $950^\circ\text{C}$ ), which leads to a very smooth QD-matrix interface, results in the appearance of phonon replicas in the PL spectrum of the annealed structures with (In,Al)As/AlAs QDs.

Let us now consider qualitatively the effect of the interface sharpness on the effective width of the  $G(\tau)$  distribution. The exciton lifetime is proportional to  $\exp(d/a + d/L)$ . Therefore,

the width of the lifetime distribution should be determined by variations of the argument  $d/a + d/L$  value for different QDs. The dispersion of a varying quantity is inversely proportional to the square root of its mean value.<sup>31</sup> Thus the width of  $G(\tau)$  should decrease with increasing value of  $d/a + d/L$ . The experimental data tend to confirm this expectation. Indeed, the effective width of the  $G(\tau)$  distribution (which is inversely proportional to  $\gamma$ ) for QDs with similar sizes decreases with increasing thickness of the diffused layer. An increase of the ratio  $d/L$  with increasing QD size for a fixed ratio  $d/a$  results in a reduction of  $d/a + d/L$  and thus in an enhancement of the  $G(\tau)$  width (a decrease of the value  $\gamma$  is shown in Table I).

#### IV. CONCLUSION

The dynamics of the exciton radiative recombination in (In,Al)As/AlAs QD ensembles with a type-I band alignment but an indirect band gap has been investigated. Due to the different dot sizes and/or QD-matrix interface sharpness, the exciton recombination dynamics shows a nonexponential decay behavior that can be described by a power-law function as a result of the superposition of multiple monoexponential PL decays with different lifetimes. The lifetime of these excitons is mostly determined by the thickness of the diffused (In,Al)As layer at the QD-matrix interface, while its dependence on the QD size is weaker. We have proposed a phenomenological equation for the distribution  $G(\tau)$  of the radiative exciton recombination times in such QD ensembles, which can describe the power-law PL decay over five orders of magnitude very well, using one fitting parameter only.

#### ACKNOWLEDGMENTS

We greatly acknowledge B. Brinkmann for help with the experiment. This work was supported by the Deutsche Forschungsgemeinschaft and the Russian Foundation of Basic Research (joint Grant No. 436 RUS 113/958/0-1 and RFBR Grants No. 10-02-00240 and No. 10-02-00077) and by NATO CLG (Grant No. 983878). T.S.S. acknowledges financial support from the DFG through Grants No. YA 65/14-1 and No. YA 65/19-1.

#### APPENDIX

The exciton wave function can be written as

$$\phi(\mathbf{r}_e, \mathbf{r}_h) = f_e(\mathbf{r}_e) f_h(\mathbf{r}_h) J(\mathbf{r}_e - \mathbf{r}_h), \quad (\text{A1})$$

where  $\mathbf{r}_e$  and  $\mathbf{r}_h$  are the coordinates of electron and hole,  $f_e$  and  $f_h$  are their wave functions in the absence of the electron-hole Coulomb interaction, and  $J(\mathbf{r}_e - \mathbf{r}_h)$  takes into account this interaction. The exciton recombination rate is proportional to  $J^2(0) | \langle f_e \nabla f_h \rangle |^2$ . If we decompose the wave functions into products of the Bloch waves times envelope wave functions  $F_e(\mathbf{r})$  and  $F_h(\mathbf{r})$  and assume that  $\nabla$  acts only on the Bloch amplitudes, then we find that the exciton recombination rate is proportional to the square of the module of the convolution of the envelopes:

$$\Gamma = \int F_e(\mathbf{r}) F_h^*(\mathbf{r}) d^3r. \quad (\text{A2})$$

To estimate this integral we assume the following form for the envelopes in the vicinity of the interface between the QD and matrix ( $z = 0$ ):

$$F_e(z) = \exp(iqz) \sum_k A(k) \exp(ikz), \quad (\text{A3})$$

$$F_h(z) = \sum_p B(p) \exp(ipz), \quad (\text{A4})$$

where  $q = \pi/a$ ,  $a$  is lattice constant, and  $A$  and  $B$  are coefficients that can be obtained from the boundary conditions. They are constants in the infinite crystal, but depend on the electron and hole momenta  $\mathbf{k}$  and  $\mathbf{p}$  in the quantum dots. The summation of these values spreads over  $k, p \sim 1/L$ , where  $L \gg a$  is the dot size (for our lens-shaped QDs  $L$  is the height of the QD). Thus we can assume that  $k, p \ll q$  and the value of the exciton recombination rate at the QD-matrix interface is determined by the integral

$$\Gamma_z = \int \exp[i(p - k + q)z] dz, \quad (\text{A5})$$

which is zero far from the interface because of the oscillating factor  $\exp(iqz)$ . We can estimate  $\Gamma_z$  at a sharp interface as

$$\Gamma_z = \int \exp[i(p - k + q)z] dz \sim \frac{1}{iq} \sim \frac{ia}{\pi}. \quad (\text{A6})$$

Integration over the dot interface leads to the estimation of  $\Gamma_z$  as the ratio of the number of atoms located at the interface to the total number of atoms in the quantum dot. The estimation of  $\Gamma_z$  at a diffused interface can be done by assuming that  $p$  and  $k$  vary smoothly with position inside the interface layer:  $p(z) = \sqrt{2m_h[E - U(z)]}$  and  $k(z) = \sqrt{2m_e[E - U(z)]}$ , where  $U(z)$  is the potential profile of a diffused interface,  $m_h$  and  $m_e$  are effective mass of heavy hole and electron, respectively. Then

$$\Gamma_z = \int_{-\infty}^{+\infty} \exp[i\{p(z) - k(z) + q\}z] dz. \quad (\text{A7})$$

To estimate  $\Gamma_z$  we consider the integrand in Eq. (A7) as a function of the complex variable  $z$ . We can displace the integration contour from the real axis  $z$  into the upper half-plane up to the nearest singularity  $z_p$  of the potential  $U(z)$ . This value is about  $id$ , where  $d$  is the characteristic thickness of the diffused interface. For

$$U(z) = \frac{U_0}{1 + \exp(-z/d)} \quad (\text{A8})$$

the value of  $z_p$  is given by  $i\pi d$ ; the actual value of  $z_p$  depends on the model for the interface. Therefore, the integral in Eq. (A7) contains the exponential factor  $\exp(iqz_p) \sim \exp(qd)$ . Evaluation of the integral [Eq. (A7)] as done similarly for Eq. (A7) in Ref. 32 results in

$$\Gamma_z \sim \frac{\exp(-qd)}{q} \sim \frac{a}{\pi} \exp\left(-\frac{d}{a}\right). \quad (\text{A9})$$

Note that the estimations in Eqs. (A5)–(A7) suppose the large size of the QD. A decrease of the QD size, e.g., of its height, leads to an increase of the electron and a decrease of the hole energies due to the size quantization as well as nonzero value of the electron and hole momenta (which is about  $\pi\hbar/L$ ). To take this fact into account, we have to add  $\pi/L$  to the exponent



in Eq. (A7), i.e., replace  $q$  with  $q + \pi/L$  in Eqs. (A7) and (A9). Then Eq. (A9) adopts the form

$$\Gamma_z \sim \frac{a}{\pi} \exp \left[ -\frac{d}{a} \left( 1 + \frac{a}{L} \right) \right]. \quad (\text{A10})$$

Taking into account that the exciton recombination rate is inversely proportional to the exciton lifetime, our estimation demonstrates that  $\tau \sim \exp(d/a + d/L)$ , i.e., an increase in thickness of the diffused layer at the QD-matrix interface results in an exponential increase of the exciton lifetime.

- 
- <sup>1</sup>A. F. van Driel, G. Allan, C. Delerue, P. Lodahl, W. L. Vos, and D. Vanmaekelbergh, *Phys. Rev. Lett.* **95**, 236804 (2005).
- <sup>2</sup>T. Berstermann, T. Auer, H. Kurtze, M. Schwab, D. R. Yakovlev, M. Bayer, J. Wiersig, C. Gies, F. Jahnke, D. Reuter, and A. D. Wieck, *Phys. Rev. B* **76**, 165318 (2007).
- <sup>3</sup>A. F. van Driel, I. S. Nikolaev, P. Vergeer, P. Lodahl, D. Vanmaekelbergh, and W. L. Vos, *Phys. Rev. B* **75**, 035329 (2007).
- <sup>4</sup>V. Zwiller, M.-E. Pistol, D. Hessman, R. Cederström, W. Seifert, and L. Samuelson, *Phys. Rev. B* **59**, 5021 (1999).
- <sup>5</sup>M. Lee, J. Kim, J. Tang, and R. M. Hochstrasser, *Chem. Phys. Lett.* **359**, 412 (2002).
- <sup>6</sup>T. Bartel, M. Dworzak, M. Strassburg, A. Hoffmann, A. Strittmatter, and D. Bimberg, *Appl. Phys. Lett.* **85**, 1946 (2004).
- <sup>7</sup>T. S. Shamirzaev, A. M. Gilinsky, A. I. Toropov, A. K. Bakarov, D. A. Tenne, K. S. Zhuravlev, C. von Borczyskowski, and D. R. T. Zahn, *JETP Lett.* **77**, 389 (2003).
- <sup>8</sup>T. S. Shamirzaev, A. V. Nenashev, and K. S. Zhuravlev, *Appl. Phys. Lett.* **92**, 213101 (2008).
- <sup>9</sup>T. S. Shamirzaev, A. M. Gilinsky, A. K. Kalagin, A. V. Nenashev, and K. S. Zhuravlev, *Phys. Rev. B* **76**, 155309 (2007).
- <sup>10</sup>L. S. Braginsky, M. Yu. Zaharov, A. M. Gilinsky, V. V. Preobrazhenskii, M. A. Putyato, and K. S. Zhuravlev, *Phys. Rev. B* **63**, 195305 (2001).
- <sup>11</sup>T. S. Shamirzaev, A. V. Nenashev, A. K. Gutakovskii, A. K. Kalagin, K. S. Zhuravlev, M. Larsson, and P. O. Holtz, *Phys. Rev. B* **78**, 085323 (2008).
- <sup>12</sup>T. S. Shamirzaev, D. S. Abramkin, A. V. Nenashev, K. S. Zhuravlev, F. Trojánek, B. Dzurňák, and P. Malý, *Nanotechnology* **21**, 155703 (2010).
- <sup>13</sup>N. Liu, J. Tersoff, O. Baklenov, A. L. Holmes Jr., and C. K. Shih, *Phys. Rev. Lett.* **84**, 334 (2000).
- <sup>14</sup>P. Offermans, P. M. Koenraad, J. H. Wolter, K. Pierz, M. Roy, and P. A. Maksym, *Phys. Rev. B* **72**, 165332 (2005).
- <sup>15</sup>E. Placidi, F. Arciprete, M. Fanfoni, F. Patella, E. Orsini, and A. Balzarotti, *J. Phys. Condens. Matter* **19**, 225006 (2007).
- <sup>16</sup>R. Panat, K. J. Hsia, and D. G. Cahill, *J. Appl. Phys.* **97**, 013521 (2005).
- <sup>17</sup>Ch. Heyn and W. Hansen, *J. Cryst. Growth* **251**, 140 (2003).
- <sup>18</sup>T. S. Shamirzaev, A. K. Kalagin, A. I. Toropov, A. K. Gutakovskii, and K. S. Zhuravlev, *Phys. Status Solidi C* **3**, 3932 (2006).
- <sup>19</sup>The recombination energy of an exciton in a QD is determined by the QD size, while photons at a certain spectral energy are contributed by QDs with similar sizes. Thus the PL band maximum corresponds to recombination in QDs with the size given by the average QD diameter. In Ref. 11 we calculated confined energy levels of QDs with different diameters as functions of the QD composition. The comparison of the measured energy of the PL maximum with the calculated optical transition energies in QDs with known average sizes allows us to determine the average composition of these QDs. The InAs fraction in the (In, Al)As QDs as a function of the substrate temperature and the growth-interruption time is given in Ref. 11.
- <sup>20</sup>B. Monemar, K. K. Shih, and G. D. Pettit, *J. Appl. Phys.* **47**, 2604 (1976).
- <sup>21</sup>H. C. Casey, D. D. Sell, and K. W. Wecht, *J. Appl. Phys.* **46**, 250 (1975).
- <sup>22</sup>J. C. Phillips, *Rep. Prog. Phys.* **59**, 1133 (1996).
- <sup>23</sup>O. Guillois, N. Herlin-Boime, C. Reynaud, G. Ledoux, and F. Huisken, *J. Appl. Phys.* **95**, 3677 (2004).
- <sup>24</sup>A. Siemiarczuk, D. Wagner, and W. R. Ware, *J. Phys. Chem.* **94**, 1661 (1990).
- <sup>25</sup>A. M. Kapitonov, A. P. Stupak, S. V. Gaponenko, E. P. Petrov, A. L. Rogach, and A. Eychmüller, *J. Phys. Chem. B* **103**, 10109 (1999).
- <sup>26</sup>C. Delerue, G. Allan, C. Reynaud, O. Guillois, G. Ledoux, and F. Huisken, *Phys. Rev. B* **73**, 235318 (2006).
- <sup>27</sup>I. S. Nikolaev, P. Lodahl, A. F. van Driel, A. F. Koenderink, and W. L. Vos, *Phys. Rev. B* **75**, 115302 (2007).
- <sup>28</sup>R. A. L. Vallée, K. Baert, B. Kolaric, M. Van der Auweraer, and K. Clays, *Phys. Rev. B* **76**, 045113 (2007).
- <sup>29</sup>The long exciton lifetimes in the (In, Al)As/AlAs QDs evidence that carriers captured in QDs recombine through photon emission only. Actually, we have demonstrated in Ref. 30 that even a small fraction of QDs containing nonradiative centers of 5% would only decrease the PL decay time down to about 1  $\mu$ s due to the long-distance transfer of the exciton energy to the nonradiative centers.
- <sup>30</sup>T. S. Shamirzaev, A. M. Gilinsky, A. K. Kalagin, A. I. Toropov, A. K. Gutakovskii, and K. S. Zhuravlev, *Semicond. Sci. Technol.* **21**, 527 (2006).
- <sup>31</sup>L. D. Landau and E. M. Lifshitz, *Statistical Physics* (Pergamon, New York, 1980).
- <sup>32</sup>E. M. Baskin, and L. S. Braginsky, *Phys. Rev. B* **50**, 12191 (1994).